

# Kinetics and rate-limiting mechanisms of dolomite dissolution at various CO<sub>2</sub> partial pressures

LIU Zaihua (刘再华)<sup>1</sup> & Dreybrodt Wolfgang<sup>2</sup>

1. Karst Dynamics Laboratory, MLR, Institute of Karst Geology, Chinese Academy of Geology Sciences, Guilin 541004, China;

2. FB1-Institut für Experimentelle Physik, Universität Bremen, Bremen 28334, Deutschland

Correspondence should be addressed to Liu Zaihua (email:zaihua\_liu@hotmail.com)

Received March 25, 2001

**Abstract** Techniques of rotating-disk and catalyst were used in investigating the kinetics of dolomite dissolution in flowing CO<sub>2</sub>-H<sub>2</sub>O system. Experiments run in the solutions equilibrated with various CO<sub>2</sub> partial pressures ( $P_{\text{CO}_2}$ ) from 30 to 100000 Pa. It shows that dissolution rates of dolomite are related with rotating speeds at conditions far from equilibrium. This was explained by modified diffusion boundary layer (DBL) model. In addition, the dissolution rates increase after addition of carbonic anhydrase (CA) to solutions, where the CA catalyzes CO<sub>2</sub> conversion. However, great differences occur among various CO<sub>2</sub> partial pressures. The experimental observations give a conclusion that the modified DBL model enables one to predict dissolution rates and their behaviour at various  $P_{\text{CO}_2}$  with satisfactory precision at least far from equilibrium.

**Keywords:** dolomite, dissolution rate, diffusion boundary layer, CO<sub>2</sub> conversion, CO<sub>2</sub> partial pressure.

The kinetics and rate-limiting mechanism of dolomite dissolution have been less extensively studied than those of calcite dissolution. Lund et al.<sup>[1]</sup> studied the dissolution of dolomite in hydrochloric acid to determine that under what conditions rate was diffusion-limited or surface reaction-limited. Herman<sup>[2]</sup> did laboratory experiments on the dissolution kinetics of dolomites. Emphasis was placed upon understanding how the effects of solvent motion and of carbonate lithology modify dissolution rates. More extensively and comprehensively, Busenberg and Plummer<sup>[3]</sup> studied the kinetics of dolomite dissolution at various temperatures and  $P_{\text{CO}_2}$ . Finally, they obtained an equation called Busenberg's equation for the net rate of dissolution as

$$R = k_1(a\text{H}^+)^n + k_2(a\text{H}_2\text{CO}_3^*)^n + k_3(a\text{H}_2\text{O})^n - k_4(a\text{HCO}_3^-), \quad (1)$$

where  $k_1$ ,  $k_2$  and  $k_3$  are forward rate constants,  $k_4$  is the backward rate constant, and  $a$  means the activity. They found that the exponent  $n$  is equal to 0.5 at temperatures below 45°C.

In 1989, Chou et al.<sup>[4]</sup> made a comparative study of the kinetics and mechanisms of dissolution of carbonate minerals. However, they found  $n = 0.75$  for dolomite dissolution, which means a more complex surface reaction.

However, the case of Lund is not common in nature, and Herman did the experiment only at very high CO<sub>2</sub> partial pressure, which is also not normal in nature<sup>[5,6]</sup>. Although the research of

Busenberg and Plummer is more extensive and comprehensive, the hydrodynamic conditions of system were not well defined in their experiments. In addition, none of these previous studies considered the role of the slow  $\text{CO}_2$  conversion reaction on the rates, which was found by us to be very important in the dissolution and precipitation of calcite<sup>[7–11]</sup>, and may also be the case for dolomite dissolution.

This study was undertaken (i) to measure the rates of dolomite dissolution far from equilibrium under various  $\text{CO}_2$  partial pressures from 30 to 100000 Pa, and (ii) to understand the role of diffusion boundary layer and the slow  $\text{CO}_2$  conversion reaction in limiting these rates by using the rotating disk technique and introducing carbonic anhydrase (CA) into solutions<sup>[8]</sup>.

## 1 Experimental

### 1.1 Materials

Dolomite disks were cored from dolomite slabs of 5 mm in thickness. Their diameter was 3.1 cm. These samples were cemented into the holder of the rotating disk apparatus. Each was then mounted to the shaft of the rotating disk equipment and polished during rotation by using waterproof silicon carbide paper. This procedure assures a continuous surface of the disk including its rim. The surface of the dolomite sample in contact with the solution was  $7.55 \text{ cm}^2$ . The mainly used dolomite was from Beijing. It was grey and of coarse microcrystalline structure. It contained 95%  $\text{CaMg}(\text{CO}_3)_2$  more. Table 1 shows its chemical analyses.

Table 1 Chemical analyses of a dolomite used in the experiment (%)

Sample	CaO	MgO	$\text{CO}_2$	P	Fe	$\text{S}/\mu\text{g} \cdot \text{g}^{-1}$	$\text{Cu}/\mu\text{g} \cdot \text{g}^{-1}$	$\text{Zn}/\mu\text{g} \cdot \text{g}^{-1}$
Beijing dolomite	30.54	21.15	46.75	0.002	0.092	32	8.2	11.8

To investigate the influence of the slow  $\text{CO}_2$  conversion reaction  $\text{CO}_2 + \text{H}_2\text{O} \rightleftharpoons \text{H}^+ + \text{HCO}_3^-$  carbonic anhydrase, an enzyme catalyzing this reaction<sup>[8]</sup> was introduced into the solution with the concentration of  $0.2 \mu\text{mol/L}$ .

To obtain solutions in equilibrium with fixed  $\text{CO}_2$  partial pressures ( $P_{\text{CO}_2}$ ),  $\text{N}_2$ - $\text{CO}_2$  gas mixtures with  $P_{\text{CO}_2} = 30, 100, 500, 1000, 5000, 10000, 20000$  and  $100000$  Pa were bubbled through the solution.

### 1.2 Experimental setup

A scheme of the experimental apparatus is shown in fig. 1. It was performed in a 1.2 L glass beaker containing 1180 mL of preset solution, which was prepared by bubbling the  $\text{CO}_2$  of relevant partial pressure into distilled water. The beaker was immersed into water that was maintained  $\pm 0.5^\circ\text{C}$  of the desired temperature. The reaction vessel was covered with Plexiglas lids with holes allowing insertion of the motorised shaft, electrodes, and a gas dispersion tube. Commercial  $\text{N}_2$ - $\text{CO}_2$  gas mixture with fixed  $P_{\text{CO}_2}$  was bubbled through a glass dispersion tube into the reaction vessel, thus providing open system conditions with respect to  $\text{CO}_2$ . The disk-shaped sample

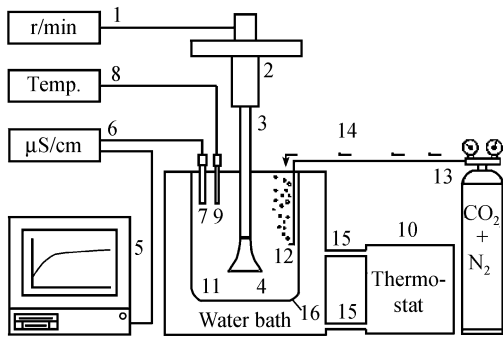


Fig. 1. Scheme of the experimental setup. 1, Controller for rotating speed; 2, motor and gear; 3, rotating shaft; 4, rotating disk; 5, computer for data acquisition; 6, conductivity meter; 7, conductivity cell; 8, thermometer; 9, temperature sensor; 10, thermostat; 11, H<sub>2</sub>O-CO<sub>2</sub> solution; 12, CO<sub>2</sub> disperser; 13, CO<sub>2</sub>+N<sub>2</sub>-supply; 14, supply tube; 15, water circulation from thermostat to waterbath cooling; 16, reactor vessel.

was centred about 4 cm above the bottom of the reaction vessel on the end of a shaft. A motor drove the shaft, and gear reducers allowed the disk to rotate in the solution at a speed varying from 0 to 3200 r/min.

Measurements of the dissolution rates were performed at a fixed rotating speed and/or concentration of carbonic anhydrase by measuring the increase in conductivity. In diluted solutions as they occur in our experiments conductivity and total hardness (TH) are related linearly by

$$\text{TH (mmol/L)} = 5.56 \times 10^{-3} \text{cond. } (\mu\text{S/cm}) - 0.01, \quad \gamma = 0.999. \quad (2)$$

Then dissolution rates of dolomite were calculated by

$$R_{\text{TH}} = (V/A)(d[\text{TH}]/dt)/2, \quad (3)$$

where  $V$  is the volume of the solution,  $A$  the area of dissolving surface and  $t$  the time. The denominator 2 means that a change of 2 mol total hardness is derived from the dissolution of only 1 mol dolomite.

The thickness of the boundary diffusion layer (DBL) is given by<sup>[12]</sup>

$$\varepsilon = 1.61(D/\nu)^{1/3}(\nu/\omega)^{1/2}, \quad (4)$$

where  $D$  is the coefficient of molecular diffusion,  $\nu$  the kinetic viscosity of water, and  $\omega$  the angular velocity in  $\text{s}^{-1}$ . In our setup  $\varepsilon = 5 \times 10^{-3}$  cm at a rotating speed of 100 r/min, and at 3000 r/min  $\varepsilon = 8.84 \times 10^{-4}$  cm. In all experimental runs the Reynolds number  $Re = r^2\omega/\nu$  ( $r$ , radius of sample) is below  $2 \times 10^5$ , such that laminar flow can be assumed<sup>[13]</sup>.

## 2 Experimental results and interpretation

### 2.1 Experimental results

The dissolution rates measured on the dolomite sample at 20 °C for three partial pressures  $P_{\text{CO}_2}$  as a function of  $\omega$  are illustrated in fig.2 by a double logarithmic plot. It was found that

$$R \propto \omega^n \quad (5)$$

with exponents  $n$  between 0.06 and 0.20. It can

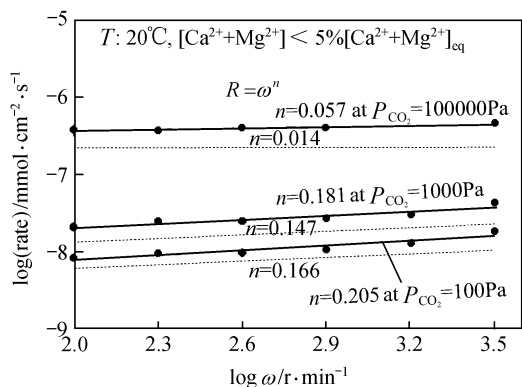


Fig. 2. Log of the experimental dissolution rates for various  $P_{\text{CO}_2}$  as a function of the log of the rotating speed in r/min (solid lines). Dotted lines are from the DBL model calculation. All curves exhibit straight lines.

be seen that the lower the  $P_{CO_2}$ , the higher the  $n$ .

This behaviour shows clearly that dissolution of dolomite is complex, because if only mass transport by diffusion is rate limiting, one would expect  $n = 0.5$ <sup>[8]</sup>.

Fig.3 further shows the factors of BCA enhancement of dolomite dissolution rates (i.e. the ratios of the rates with and without BCA under otherwise identical conditions) at various  $P_{CO_2}$  and rotating speeds.

It can be seen that at low  $P_{CO_2}$  ( $\leq 5000$  Pa) there is significant change in the rates upon

addition of BCA, with factors of BCA enhancement from 1.29—3.07. Moreover there is a peak value in the middle, which can also be predicted by the DBL model and discussed below, though there are some differences in quantity (fig. 3). For high  $P_{CO_2}$  ( $> 5000$  Pa), however, the BCA enhancement of the rates is smaller, even undetectable (factor  $\leq 1$ ) due to prevention of the more remarkable decrease in dissolution rate with time. In addition, it can also be seen that the influence of CA on dolomite dissolution is larger at low rotating speed (or thicker boundary layer) than that at high speed. Measurements were performed also at 10°C. It seems that low temperature is not favourable to detect the role of CA on the rates, i.e., the factor of CA enhancement is smaller at low temperature.

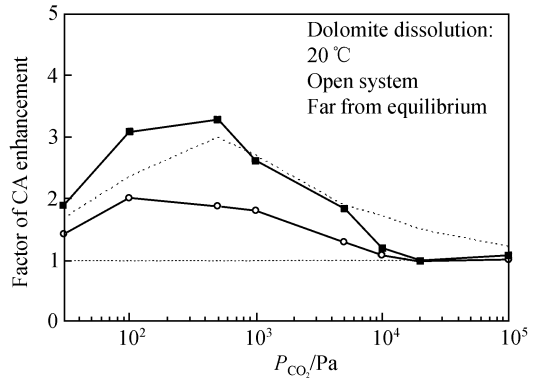


Fig. 3. Factor of carbonic anhydrase (CA) enhancement as a function of  $P_{CO_2}$  at rotating speeds of 3000 and 100 r/min. Dotted line is from the DBL-model calculation for 3000 r/min (or  $\epsilon = 9 \times 10^{-4}$  cm).  $\circ$ , 3000 r/min, 0.2  $\mu\text{mol/L}$  CA;  $\blacksquare$ , 100 r/min, 0.2  $\mu\text{mol/L}$  CA.

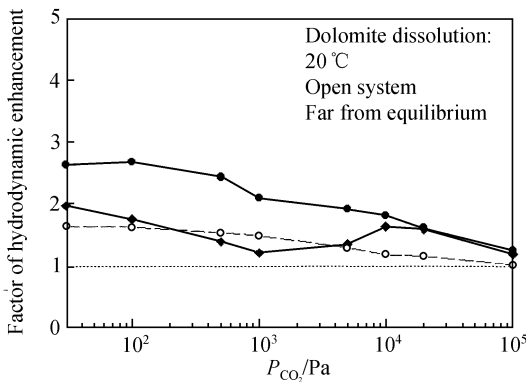


Fig. 4. Factor of hydrodynamic enhancement as a function of  $P_{CO_2}$  with/without carbonic anhydrase (0.2  $\mu\text{mol} \cdot \text{L}^{-1}$ ). Dotted line is from the DBL-model calculation for the case without carbonic anhydrase.  $\bullet$ , No CA, 3000  $\text{r} \cdot \text{min}^{-1}$ /100  $\text{r} \cdot \text{min}^{-1}$ ;  $\blacklozenge$ , with 0.2  $\mu\text{mol/L}$  CA, 3000  $\text{r} \cdot \text{min}^{-1}$ /100  $\text{r} \cdot \text{min}^{-1}$ ;  $\circ$ , no CA, 3000  $\text{r} \cdot \text{min}^{-1}$ /100  $\text{r} \cdot \text{min}^{-1}$  (DBL model).

Fig.4 further shows the factors of hydrodynamic enhancement of dolomite dissolution rates between 3000 and 100 r/min at various  $P_{CO_2}$  with/without BCA. It can be seen again that dolomite dissolution at low  $P_{CO_2}$  is more sensitive to hydrodynamic change than that at high  $P_{CO_2}$ . In addition, the sensitivity decreases after addition of carbonic anhydrase to solution.

These results show that some changes in rate-limiting mechanism of dolomite dissolution occur at low  $P_{CO_2}$ . Therefore

one has to be cautious to conclude from the experiments with high  $P_{\text{CO}_2}$  ( $> 5000$  Pa) to the dissolution processes in nature, which usually occur at low  $P_{\text{CO}_2}$  ( $< 5000$  Pa).

## 2.2 Interpretation of the experimental observations

Chou et al.<sup>[4]</sup> found that the two-step reaction mechanism proposed by Busenberg and Plummer<sup>[3]</sup> cannot explain their fractional reaction order (0.75), which is likely due to a more complex surface reaction. But it seems, if the limiting of diffusion boundary layer and the effect of

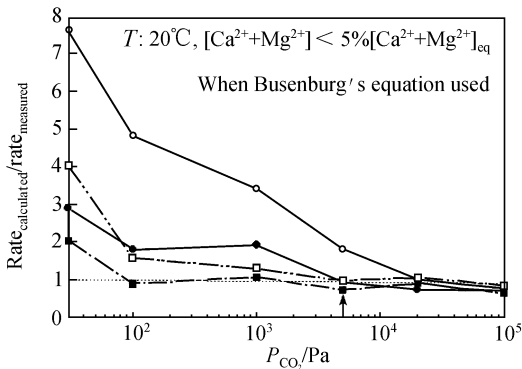


Fig. 5. Ratio of calculated rates by Busenberg's equation to measured rates at rotating speeds of 3000 and 100 r/min with/without carbonic anhydrase (CA) as a function of  $P_{\text{CO}_2}$ . ●, 3000 r/min; ○, 100 r/min; ■, 3000 r/min with 0.2  $\mu\text{mol/L}$  CA; □, 100 r/min with 0.2  $\mu\text{mol/L}$  CA.

slow  $\text{CO}_2$  conversion reaction were not considered, that the calculated rates by Busenberg's equation are closer to the measured rates by this investigation. Fig. 5 shows the ratio of the calculated rates to measured rates at different rotating speeds and with/without carbonic anhydrase as a function of  $P_{\text{CO}_2}$ . As shown in fig.5, the Busenberg's equation is valid only at high  $P_{\text{CO}_2}$  ( $> 5000$  Pa), where, according to our experimental results above, both the hydrodynamic and carbonic anhydrase enhancement are very small.

In order to interpret this further, we make use of the DBL model for calcite dissolution by Dreybrodt and Buhmann<sup>[10]</sup>, that considers the concerted action of three processes determining the rate of dissolution simultaneously. The three processes are (i) the kinetics of the heterogeneous surface reaction of  $\text{CaCO}_3$  released from the crystalline surface into the solution, using the rate equation established by Plummer et al.<sup>[14]</sup>; (ii) the kinetics of the slow  $\text{CO}_2$  conversion reaction<sup>[15,16]</sup>; and (iii) the mass transport of the dissolved species.

Now, what we need is just to replace the PWP equation by Busenberg's equation<sup>[3]</sup> in the DBL model to get a modified DBL model especially for dolomite dissolution.

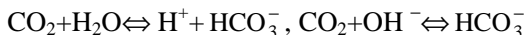
In the following is a short description of the basic assumptions of the modified DBL model, as we will use it to interpret the experimental data.

Fig. 6 shows the concept model of the DBL with thickness  $\epsilon$ , separating the dolomite surface from the turbulent bulk of thickness  $\delta$ . In the region of the bulk, complete mixing is assumed, such that no concentration gradients can be built up. This can be modelled by assuming the turbulent diffusion coefficient  $D_t$  to be higher by a factor of  $10^6$  than the coefficient of molecular diffusion, which describes mass transfer in the DBL. The flux  $F$  of dolomite dissolution is given by the Busenberg's equation using the activities of the species at the surface of the solid phase. For sto-

chiometric reasons this flux must be equal to the total amount of  $\text{CO}_2$  converted to  $\text{H}^+ + \text{HCO}_3^-$  in a column with area of  $1 \text{ cm}^2$  covering the region from  $-\delta \leq z \leq \varepsilon$ . This is given by

$$F_{\text{CO}_2} = \int_{-\delta}^{\varepsilon} R_{\text{CO}_2}(z) dz, \tag{6}$$

where  $R_{\text{CO}_2}$  is the change of the  $\text{CO}_2$  concentration in time, resulting from two elementary reactions, occurring simultaneously.



The rate constants of these reactions are well known<sup>[11]</sup>.

Using these boundary conditions the equations of mass transport can be solved numerically<sup>[11]</sup>.

In the following we give the results obtained employing this modified model. In the first step we have calculated the dissolution rates for the experiments as depicted in figs. 2 and 3. The DBL thickness  $\varepsilon$  was obtained from eq. (4). For the experimental conditions with an area of the disk of  $7.55 \text{ cm}^2$  and a total volume of the solution of  $1180 \text{ cm}^3$ , the thickness  $\delta$  of the turbulent core is  $156 \text{ cm}$ . Fig. 7 depicts as lines with the theoretical dissolution rates as a function of  $\varepsilon$  for the various  $\text{CO}_2$  partial pressures as used in the experiment. The data points represent the experimental data in figs. 2 and 3; but they are divided by a factor of about 1.5 (the average of the ratios of experimental rates to theoretical rates) to fit to the theoretical curves consistently. The reason for this behaviour is not very clear. One reason may be that owing to the roughness of the surface the effective surface for dissolution is higher than the geometrical one. Considering this, division of the experimental data by 1.5 is feasible, to render them comparable to the predictions of the DBL-model. Fig. 7 gives the evidence that the experimental data and the model predictions are in

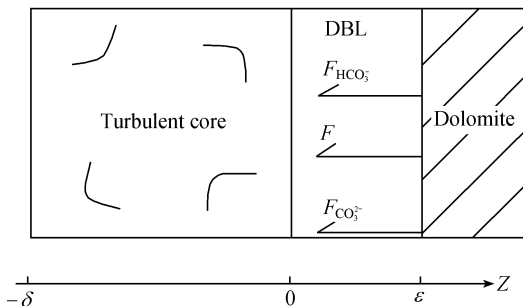


Fig. 6. The geometry of the modified DBL-model. The DBL extends from  $z = 0$  to  $z = \varepsilon$ . The well mixed core extends from  $z = 0$  to  $z = -\delta$ . The arrows denote fluxes of  $\text{CO}_3^{2-}$ ,  $\text{HCO}_3^-$ , and dissolution from the mineral surface. Note that  $F$  is given by the Busenberg's equation (eq. (1)) employing the activities of the species at  $z = \varepsilon$ .

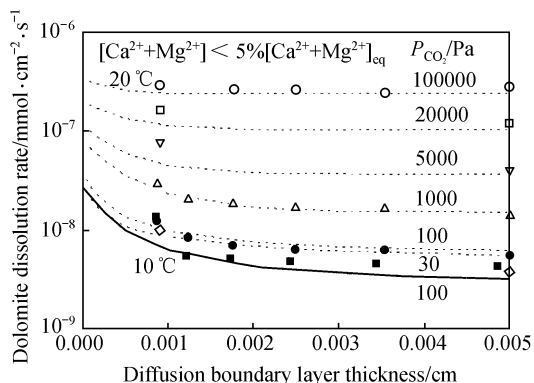


Fig. 7. Dissolution rates versus the DBL-thickness  $\varepsilon$  for various  $P_{\text{CO}_2}$ . The symbols represent the experimental points divided by 1.5 account of the larger actual effective surface area than the geometric surface area. The lines are obtained from the modified DBL model. Lines, modeled by the DBL model; points, measured by rotating disk experiments ( $R_{\text{exp}}/1.5$ ).

satisfactory agreement. The model also shows clearly that the rates depend mainly on  $\varepsilon$  if the  $\text{CO}_2$  pressure is low, whereas almost no dependence on  $\varepsilon$  is predicted for  $P_{\text{CO}_2} > 5000$  Pa and at  $\varepsilon > \sim 1 \times 10^{-3}$  cm, which is the range in this study.

To elucidate this behaviour we used the modified theoretical DBL-model to calculate the concentration profiles in the boundary layer. Figs. 8(a) and (b) illustrate these profiles of  $\text{H}^+$ ,  $\text{HCO}_3^-$  and  $\text{CO}_3^{2-}$ , and  $P_{\text{CO}_2}$  across the boundary layer for  $P_{\text{CO}_2} = 100$  and 20000 Pa, at  $\varepsilon = 0.005$  cm. The boundary to the bulk is at the left-hand side at  $z = 0$ . The units for the different species are denoted at the corresponding ordinates. From the profiles one reads that  $\text{H}^+$  and  $\text{CO}_2$  migrate from the bulk towards the solid phase on the right-hand side whereas  $\text{CO}_3^{2-}$  and  $\text{HCO}_3^-$  diffuse towards the bulk. The fluxes of these species are given by the first law of Fick as

$$F = -D(\partial c / \partial z), \quad (7)$$

where  $c$  is the concentration of the corresponding species. Therefore the fluxes can be read from the slopes of the profiles. Spatial changes of the slopes must be interpreted as changes of fluxes, which are accompanied by chemical reactions in which the corresponding species is involved.

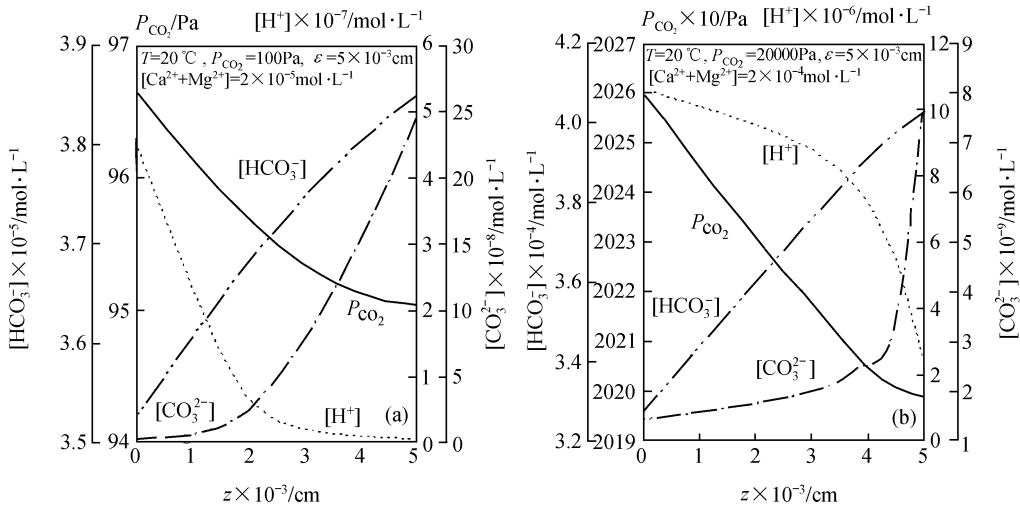


Fig. 8. Profiles of  $P_{\text{CO}_2}$ ,  $[\text{H}^+]$ ,  $[\text{HCO}_3^-]$  and  $[\text{CO}_3^{2-}]$  across the diffusion boundary layer for  $\varepsilon = 0.005$  cm, when  $P_{\text{CO}_2} = 100$  Pa (a) and  $P_{\text{CO}_2} = 20000$  Pa (b).

At the calcite surface ( $z = 0.005$  cm) due to the dissolution process there is a flux of  $\text{HCO}_3^-$  and  $\text{CO}_3^{2-}$  towards the bulk. In order to keep the saturation index with respect to the relevant mineral sufficiently low,  $\text{CO}_3^{2-}$  must react with  $\text{H}^+$  to form  $\text{HCO}_3^-$ . Due to mass transport by diffusion towards the bulk the flux of  $\text{HCO}_3^-$  (given by the slope of the profile) increases slightly for two reasons: firstly  $\text{CO}_3^{2-}$  ions react with  $\text{H}^+$  ions diffusing from the bulk into the DBL and

secondly close to the solid phase boundary, CO<sub>2</sub> migrating from the bulk reacts with H<sup>+</sup>, which is then consumed by the reaction with CO<sub>3</sub><sup>2-</sup>.

If the DBL is sufficiently thin, the time for the species to migrate across the layer becomes so short that the chemical reactions cannot complete in the layer. In this case, quantity of CO<sub>2</sub> conversion is very small, and the molecular diffusion will be more important in the layer. This explains why there is a variation of the dissolution rates with decreasing ε.

To further reveal the difference in rate-limiting mechanisms between high and low P<sub>CO<sub>2</sub></sub>, we plotted the ratio of [CO<sub>2</sub>]<sub>aq</sub>/[H<sub>2</sub>CO<sub>3</sub>] as a function of distance to the bulk for the layer, as depicted in fig. 9(a). It can be clearly seen that the ratio at low P<sub>CO<sub>2</sub></sub> (curve 1) is much higher than that at high P<sub>CO<sub>2</sub></sub> (curve 2), especially near dolomite surface. Theoretically, if CO<sub>2</sub> conversion was fast enough and not rate-limiting, the ratio of [CO<sub>2</sub>]<sub>aq</sub>/[H<sub>2</sub>CO<sub>3</sub>] would be close to equilibrium value of about 400 at 20°C<sup>[11]</sup>. The larger the ratio, the stronger the CO<sub>2</sub> conversion control on rate. So, the addition of CA to solution can enhance the dissolution of dolomite a lot at low P<sub>CO<sub>2</sub></sub>, but the enhancement becomes much smaller at high P<sub>CO<sub>2</sub></sub>. This behaviour is just the opposite to the case of calcite dissolution (fig. 9(b)), where the addition of CA to solution can enhance the dissolution rate a lot at high P<sub>CO<sub>2</sub></sub>, but the enhancement becomes much smaller at low P<sub>CO<sub>2</sub></sub><sup>[8]</sup>.

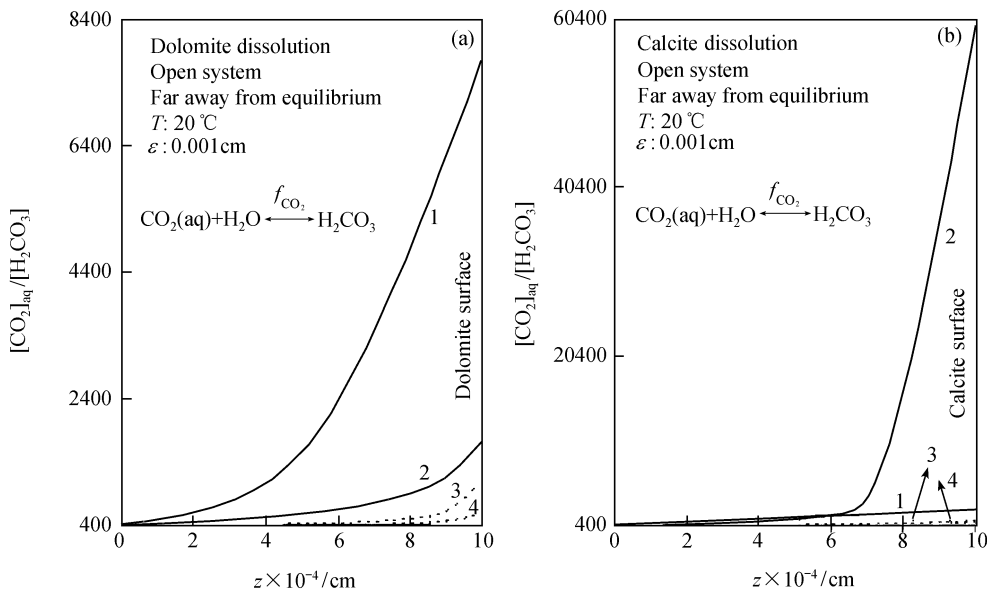


Fig. 9. Ratio of [CO<sub>2</sub>]<sub>aq</sub>/[H<sub>2</sub>CO<sub>3</sub>] as a function of distance to the bulk for the layer when dolomite (a) and calcite (b) dissolution happens. Here f<sub>CO<sub>2</sub></sub> is the multiplier of rate increase of the CO<sub>2</sub> conversion reaction. 1, Low P<sub>CO<sub>2</sub></sub> at 100 Pa; 2, high P<sub>CO<sub>2</sub></sub> at 10000 Pa; 3, 1 after f<sub>CO<sub>2</sub></sub> =250; 4, 2 after f<sub>CO<sub>2</sub></sub> =30.

### 3 Conclusions

We have measured, by use of the rotating disk technique, dissolution rates of dolomite as they occur in natural waters not only for low  $P_{\text{CO}_2}$ , but also for high  $P_{\text{CO}_2} > 5000$  Pa, which are not likely to occur in nature.

The aim of these experiments is to reveal the role of the laminar diffusion boundary layer, which separates the surface of the dissolving mineral from the well-mixed bulk of the solution. Our results give a clear evidence, that the diffusion boundary layer across which mass transport must be affected by molecular diffusion can reduce the rates significantly. Furthermore, the slow reaction  $\text{CO}_2 + \text{H}_2\text{O} \rightleftharpoons \text{H}^+ + \text{HCO}_3^-$  plays a significant role, which so far has not been sufficiently considered in most problems dealing with dissolution or precipitation of dolomite by many researchers in this field<sup>[2-4,17-21]</sup>. Moreover, we have found that in the presence of a diffusion boundary layer the rate-limiting mechanism of dolomite dissolution is different between low  $P_{\text{CO}_2}$  ( $< 5000$  Pa) and high  $P_{\text{CO}_2}$  ( $> 5000$  Pa). It changes from mixed-control of diffusion boundary layer (mass transport control) and  $\text{CO}_2$  conversion at low  $P_{\text{CO}_2}$ , to mainly surface reaction control at high  $P_{\text{CO}_2}$ , at least under our experimental conditions. The good agreement of the predictions of the DBL model with the experimentally observed data gives confidence that reliable estimations can be made at least far from equilibrium.

This has important consequences. Many dissolution experiments using the rotating disk or stirring technique have employed a partial pressure  $P_{\text{CO}_2} > 5000$  Pa<sup>[4,19]</sup>. In this case rates are determined mainly by surface reaction, and no valid conclusion can be drawn on the role of mass transport and/or  $\text{CO}_2$  conversion in dissolution mechanisms of the mineral.

At last, by comparison between dolomite and limestone, we obtain the following conclusions:

(i) The initial dissolution rates of dolomite are 2.5—7.5 times lower than those of limestone, and the lower the  $P_{\text{CO}_2}$ , the higher the difference;

(ii) For limestone, the effect of carbonic anhydrase (CA) on dissolution rates is mainly at high  $P_{\text{CO}_2}$  ( $> 5000$  Pa), with about 10 times increase in rates after the addition of the CA. For dolomite, however, the influence of CA is mainly at low  $P_{\text{CO}_2}$  ( $< 5000$  Pa). Moreover, the increase in rates after the addition of the CA is much less, with only a factor of about 3.

(iii) The dissolution of both dolomite and limestone is sensitive to the hydrodynamic change, but only at low  $P_{\text{CO}_2}$  ( $< 5000$  Pa).

These findings further confirm that the behavior of dolomite dissolution is due to a more complex surface reaction. It may explain why great differences in karstification and water storage

occur between dolomite and limestone.

**Acknowledgements** This work was supported by the National Natural Science Foundation of China (Grant No. 40073026), the Ministry of Land and Resources of China (Grant No. 9806), the Ministry of Science and Technology of China (Special Research Project for Social Commonweal) (Grant No. 164), the Natural Science Foundation of Guangxi Autonomous Region, China (Grant No. 9824021) and Bremen University of Germany.

## References

1. Lund, K., Fogler, H. S., McCune, C. C., Acidization—I. The dissolution of dolomite in hydrochloric acid, *Chem. Eng. Sci.*, 1973, 28: 691—700.
2. Herman, J. S., The dissolution kinetics of calcite, dolomite and dolomite rocks in carbon dioxide water system, PH. D. Thes., Pennsylvania State Univ., 1982.
3. Busenberg, E., Plummer, L. N., The kinetics of dissolution of dolomite in CO<sub>2</sub>-H<sub>2</sub>O systems at 1.5 to 65°C and 0 to 1 atm P<sub>CO<sub>2</sub></sub>, *Amer. Jour. Sci.*, 1982, 282: 45—78.
4. Chou, L., Garrels, R. M., Wollast, R., Comparative study of the kinetics and mechanisms of dissolution of carbonate minerals, *Chem. Geol.*, 1989, 78: 269—282.
5. Liu, Z., Yuan, D., He, S. et al. Geochemical features of the geothermal CO<sub>2</sub>-water-carbonate rock system and analysis on its CO<sub>2</sub> Sources, *Science in China, Series D*, 2000, 43(6): 569—576.
6. Shangguan, Z., Bai, C., Sun M., Mantle-derived magmatic gas releasing features at the Rehai area, Tengchong County, Yunnan Province, China, *Science in China, Series D*, 2000, 43(2): 132—140.
7. Dreybrodt, W., Lauckner, J., Liu, Z. et al., The kinetics of the reaction CO<sub>2</sub>+ H<sub>2</sub>O⇒H<sup>+</sup>+ HCO<sub>3</sub><sup>-</sup> as one of the rate limiting steps for the dissolution of calcite in the system H<sub>2</sub>O-CO<sub>2</sub>-CaCO<sub>3</sub>, *Geochim. Cosmochim. Acta*, 1996, 60: 3375—3381.
8. Liu, Z., Dreybrodt, W., Dissolution kinetics of calcium carbonate minerals in H<sub>2</sub>O-CO<sub>2</sub> solutions in turbulent flow: the role of the diffusion boundary layer and the slow reaction H<sub>2</sub>O+CO<sub>2</sub>↔H<sup>+</sup>+HCO<sub>3</sub><sup>-</sup>, *Geochim. Cosmochim. Acta*, 1997, 61: 2879—2889.
9. Dreybrodt, W., Eisenlohr, L., Madry, B. et al., Precipitation kinetics of calcite in the system CaCO<sub>3</sub>-H<sub>2</sub>O-CO<sub>2</sub>: The conversion to CO<sub>2</sub> by the slow process H<sup>+</sup>+HCO<sub>3</sub><sup>-</sup> ⇒ CO<sub>2</sub> + H<sub>2</sub>O as a rate limiting step, *Geochim. Cosmochim. Acta*, 1997, 61: 3897—3904.
10. Dreybrodt, W., Buhmann, D., A mass transfer model for dissolution and precipitation of calcite from solutions in turbulent motion, *Chem. Geol.*, 1991, 90: 107—122.
11. Dreybrodt, W., *Processes in Karst Systems*, Springer Series in Physical Environment, Heidelberg: Springer, 1988.
12. Levich, V. G., *Physicochemical Hydrodynamics*, Englewood Cliffs: Prentice-Hall, 1962.
13. Pleskov, Y. V., Filinovskii, V. Y., *The Rotating Disc Electrode*, New York: Consultants Bureau, 1976.
14. Plummer, L. N., Wigley, T. M. L., Parkhurst, D. L., The kinetics of calcite dissolution in CO<sub>2</sub>-water systems at 5—60°C and 0.0—1.0 atm CO<sub>2</sub>, *Am. J. Sci.*, 1978, 278: 179—216.
15. Kern, M. D., The hydration of carbon dioxide, *J. Chem. Educ.*, 1960, 37: 14—23.
16. Usdowski, E., Reactions and equilibria in the systems CO<sub>2</sub>-H<sub>2</sub>O and CaCO<sub>3</sub>-CO<sub>2</sub>-H<sub>2</sub>O, A review, *N. J. Mineral Abh.*, 1982, 144: 148—171.
17. Arvidson, R. S., Mackenzie, F. T., The dolomite problem: the control of precipitation kinetics by temperature and saturation state, *Amer. Jour. Sci.*, 1999, 299: 257—288.
18. Gautelier, M., Oelkers, E. H., Schott, J., An experimental study of dolomite dissolution rates as a function of pH from -0.5 to 5 and temperature from 25 to 80°C, *Chem. Geol.*, 1999, 157: 13—26.
19. Herman, J. S., White, W. B., Dissolution kinetics of dolomite: effect of lithology and fluid velocity, *Geochim. Cosmochim. Acta*, 1985, 49: 2017—2026.
20. Orton, R., Unwin, P. R., Dolomite dissolution kinetics at low pH: a channel-flow study, *J. Chem. Soc., Faraday Trans.*, 1993, 89: 3947—3954.
21. Vasconcelos, C. O., McKenzie, J. A., Bernasconi, S. et al., Microbial mediation as a possible mechanism for natural dolomite formation at low temperature, *Nature*, 1995, 337: 220—222.